REPORT DOCUMENTATION PAGE

1. REPORT DATE (DD-MM-YYYY)	2. REPORT TYPE	3. DATES COVERED (From - To)
08-12-2005	Technical Paper	

4. TITLE AND SUBTITLE	5a. CONTRACT NUMBER
Laser-Driven Mini-Thrusters (PREPRINT)	5b. GRANT NUMBER
	5c. PROGRAM ELEMENT NUMBER

6. AUTHOR(S)	5d. PROJECT NUMBER
Enrique Sterling, Jun Lin, John Sinko, Lisa Kodgis, Simon Porter and Andrew V. Pakhomov	4847
(Dept of Physics, Univ of Alabama Huntsville);	5e. TASK NUMBER
C. William Larson and Franklin B. Mead, Jr. (AFRL/PRSP)	0159
	5f. WORK UNIT NUMBER

7. PERFORMING ORGANIZATION NAME(S) AND ADDRESS(ES)	8. PERFORMING ORGANIZATION REPORT NUMBER
Air Force Research Laboratory (AFMC) AFRL/PRSP 10 E. Saturn Blvd. Edwards AFB CA 93524-7680	AFRL-PR-ED-TP-2005-490

9. SPONSORING / MONITORING AGENCY NAME(S) AND ADDRESS(ES)	10. SPONSOR/MONITOR'S ACRONYM(S)
Air Force Research Laboratory (AFMC) AFRL/PRS 5 Pollux Drive Edwards AFB CA 93524-70448	11. SPONSOR/MONITOR'S NUMBER(S) AFRL-PR-ED-TP-2005-490

12. DISTRIBUTION / AVAILABILITY STATEMENT

Approved for public release; distribution unlimited

14. ABSTRACT
Laser-driven mini-thrusters were studied using Delrin® and PVC (Delrin® is a registered trademark of DuPont) as propellants. TEA CO_2 laser ($\lambda = 10.6$ μm) was used as a driving laser. Coupling coefficients were deduced from two independent techniques: force-time curves measured with a piezoelectric sensor and ballistic pendulum. Time-resolved ICCD images of the expanding plasma and combustion products were analyzed in order to determine the main process that generates the thrust. The measurements were also performed in a nitrogen atmosphere in order to test the combustion effects on thrust. A pinhole transmission experiment was performed for the study of the cut-off time when the ablation/air breakdown plasma becomes opaque to the incoming laser pulse.

15. SUBJECT TERMS

16. SECURITY CLASSIFICATION OF:			17. LIMITATION OF ABSTRACT	18. NUMBER OF PAGES	19a. NAME OF RESPONSIBLE PERSON Dr. Franklin B. Mead, Jr.
a. REPORT	b. ABSTRACT	c. THIS PAGE	A	13	19b. TELEPHONE NUMBER (include area code) (661) 275-5929
Unclassified	**Unclassified**	**Unclassified**			

Laser-Driven Mini-Thrusters

Enrique Sterling, Jun Lin, John Sinko, Lisa Kodgis, Simon Porter, and
Andrew V. Pakhomov

Department of Physics, The University of Alabama in Huntsville, Huntsville, AL 35899, USA

C. William Larson and Franklin B. Mead, Jr.

Propulsion Directorate, Air Force Research Laboratory, Edwards AFB, CA 93524-7680, USA

Abstract. Laser-driven mini-thrusters were studied using Delrin® and PVC (Delrin® is a registered trademark of DuPont) as propellants. TEA CO_2 laser ($\lambda = 10.6$ μm) was used as a driving laser. Coupling coefficients were deduced from two independent techniques: force-time curves measured with a piezoelectric sensor and ballistic pendulum. Time-resolved ICCD images of the expanding plasma and combustion products were analyzed in order to determine the main process that generates the thrust. The measurements were also performed in a nitrogen atmosphere in order to test the combustion effects on thrust. A pinhole transmission experiment was performed for the study of the cut-off time when the ablation/air breakdown plasma becomes opaque to the incoming laser pulse.

INTRODUCTION

The objective of this study was to test various polymer propellants installed within laser-thruster prototypes, which we will call "mini-thrusters". The major scheme for the study was to attempt real-time parallel measurements using piezoelectric force sensor and intensified charge-coupled device (ICCD) imaging system [1-4], in order to determine the dominant mechanisms of thrust generation and relevant propulsive parameters, such as impulse and coupling coefficient.

The motivation for present study came out of several previous efforts. First of all, it was demonstrated that the addition of solid Delrin to both Myrabo Laser Lightcraft [5] and bell-shaped German lightcraft [6, 7] led to substantial improvement of lightcraft performance. Second, this study was done as a continuation of previous research on air pressure effect on laser-generated thrust using a TEA CO_2 laser; the pressures were varied in 3.5 mTorr – 1 atm range [2, 3]. In this study a ballistic pendulum technique was developed to differentiate between the contributions to coupling coefficient from laser-induced air breakdown versus direct ablation of propellant. However, in spite of reliable data on imparted momentum, ballistic pendulum cannot provide time-resolved force measurement. In order to record the timeline of thrust evolution in detail, various piezoelectric force sensors were used which led to experimental values of specific impulse, coupling coefficient and efficiency. The impulse determined from integration force-time curves was compared to the data derived from the ballistic pendulum. In parallel, images of laser-ablated propellant were recorded with an ICCD camera. The laser pulse energy deposition, the plasma formation and evolution, the shock wave

expansion and combustion were imaged and compared with the force-time curves. The combination of these experimental techniques led to a better understanding of the dominant process of thrust generation.

EXPERIMENTAL TECHNIQUES

A transverse excited atmospheric (TEA) CO_2 laser (Lumonics TEA 100-2), emitting single 300-ns-wide pulses with 2 μs low-intensity tails at a wavelength of 10.6 μm was focused using a 15 cm convex gold-plated mirror (R = 5 m) on the surface of the test polymer (White and Black Delrin®, PVC) pellets of diameter 0.95 cm and length 0.5 cm. The pellets were installed inside aluminum thrusters of two different expansion ratios (16:1 and 8:1) (Figures 1a and b). Figure 1a shows an actual combustion plume that developed under laser irradiation. Figure 1c shows the "off-pendulum" experimental arrangement, where the thruster was attached to the pendulum while the sensor was fixed to a separate stand. We also attempted to use the on-pendulum arrangement, when the sensor was mounted on the pendulum. Laser output energy set to 10 J was monitored using a Scientech 365 energy/power meter connected to a Scientech 380202 calorimeter.

a). Pendulum-mounted thruster.

b). 16:1 and 8:1 thrusters.
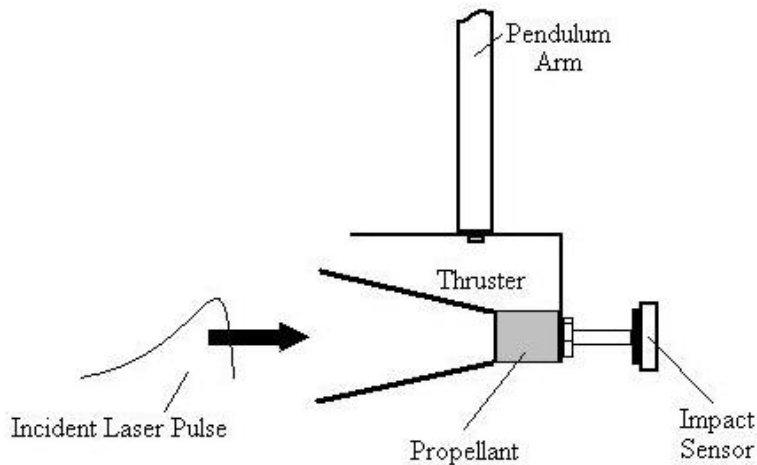
c). Experimental setup.

FIGURE 1. Experimental setup and Mini- thrusters.

Force-Time Curve Measurements

The force-time curves were measured using various models of quartz piezoelectric force sensors (PCB Piezotronics 209C01, 209M63) and impact sensors (PCB Piezotronics 200B01, 200B02)) connected to an oscilloscope (Tektronix TDS 680B) via a signal conditioner. The force-time curve $F(t)$ was in turn integrated to obtain net impulse (I), and thus, coupling coefficient (C_m), defined as:

$$C_m \equiv \frac{1}{E} \int_0^{t_0} F(t)dt = \frac{I}{E},$$ (1)

where E is pulse energy.

Ballistic Pendulum

The second technique used a ballistic pendulum [2, 3], usually with the thruster mounted on the pendulum. The pendulum was allowed to oscillate freely when struck by the laser pulse. The angular displacement was marked using a He-Ne laser beam reflected off the pendulum; the spot position was recorded using a video camera.
The coupling coefficient derived from this measurement is given by [2, 3]:

$$C_m = \frac{mgl_c T}{2\pi Er} \sqrt{2(1 - \cos\theta)}$$ (2)

where m is the pendulum's total mass, l_c is the pivot point-center of mass distance, T is the oscillation period, r is the thruster-pivot point length, and θ is the pendulum's angular displacement. One may rewrite the pendulum's angular displacement θ in terms of displacement of the He-Ne laser's reflected beam. By taking the small angle approximation to the tangent of the angle:

$$\theta \approx \tan\theta = \frac{x}{2D}$$ (3)

where x is the displacement of the reflected He-Ne laser beam spot and D is the distance from the pendulum to the plane of measurement (see Figure 2).
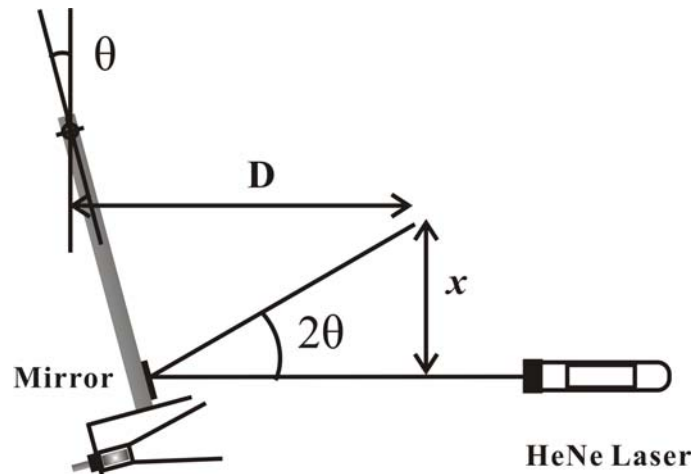
FIGURE 2. The geometry of the pendulum displacement measurements.

ICCD Imaging

Following to the imaging technique developed in a previous work [4], images were taken of the expanding plasma and vapor plumes on the surface of the propellant pellets alone, using a Princeton Instruments 576G ICCD camera and Princeton Instruments ST130 controller. A Princeton Instruments PG200 delay generator, triggered using an ultrafast pyroelectric sensor (Molectron P5-01), was used with ICCD to capture the exhaust images in its various evolution states. For details on ICCD imaging setup, please see Ref. 4. Since the force/impact sensors used resolved the force temporally with a 5 - 8 μs rise time, it was possible to compare the plasma and combustion plume evolution images with the corresponding force-time curves, including times characteristic to the peak of thrust.

Combustion Tests

In order to test if the combustion of propellant has a contribution to the thrust, the thruster was placed inside a vacuum chamber filled with nitrogen to 1 atm. The vacuum chamber was evacuated using a HOVAC Turbo-60E roughing/turbo pump down to 4×10^{-3} Torr, vacuum levels were measured using a Teledyne TV-4DM tube sensor connected to a Kurt Lesker IG 4400 controller. Impulse was measured for varying nitrogen pressures and then compared to experiments in air.

Temporal Resolution of Plasma Shielding

Delrin and Aluminum targets with pinholes drilled along the axis (pinhole diameter ≈ 0.5 mm), were used to measure transmitted pulse energy as a function of time with a Molectron P5-01 ultrafast pyroelectric detector. The laser pulse, with diameter of 1 cm and 7 J pulse energy was focused on the target surface. As it is shown in Figure 3, the transmitted light passed through the pinhole and a similar opening in the supporting screw. Using the free-propagating pulse as a reference, temporal energy profiles were measured for transmission through the pinholes for the various propellants.
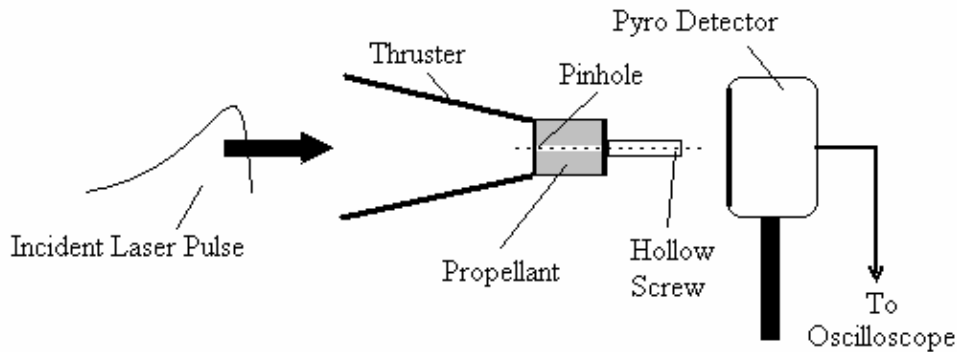
FIGURE 3. Schematics of the transmission experiment.

RESULTS AND DISCUSSION

Impulse Measurements

As it has been described above, the imparted impulses were deduced from two independent techniques. The coupling coefficients were calculated using Equation (2) in the case of the pendulum, and by integrating the force-time curve (Equation 1), for the force sensor case. The data of black Delrin with an 8:1 thruster is shown in Table 1 as an example. Force-time curves were obtained for the sensor mounted on the pendulum and off the pendulum.

TABLE 1. Pendulum and sensor impulse values. 8:1 thruster, black Delrin, E = 6.8 J.

Technique		Impulse (dyne-s)	C_m (dyne/W)
Force Sensor	*on-pendulum*	320	47
	off-pendulum	565	83
Ballistic Pendulum		355	52

Note that the impulse derived from the force sensor measurement off-pendulum is almost *twice* the actual value measured on the ballistic pendulum and with the sensor on-pendulum. The latter two numbers appear close within 10% margin. It is assumed that the difference between on- and off-pendulum data is due to addition of recoil momentum in the latter configuration, which would double the impulse in the case of a perfectly elastic collision. Of course, there is no recoil in the on-pendulum case, since the sensor rides freely together with the pendulum. The difference between these two measurements is illustrated in Figure 4, where both impulse curves reach the same peak force, but the time base for off-pendulum configuration is about twice as wide.

Figure 4 shows the difference between the force curves for on- and off-pendulum cases. The off-pendulum curve is regular and symmetric. The on-pendulum curve has

shorter rise time, some irregular structure of peak value and 15 μs early onset. The reasons for all mentioned features for on-pendulum curve are not clear. A possible explanation is that when the sensor is placed in accelerating frame of reference, its signal shows different temporal characteristics, *i.e.* the sensor is merely can not work properly under accelerations. However, further study is needed for a better understanding of this effect.
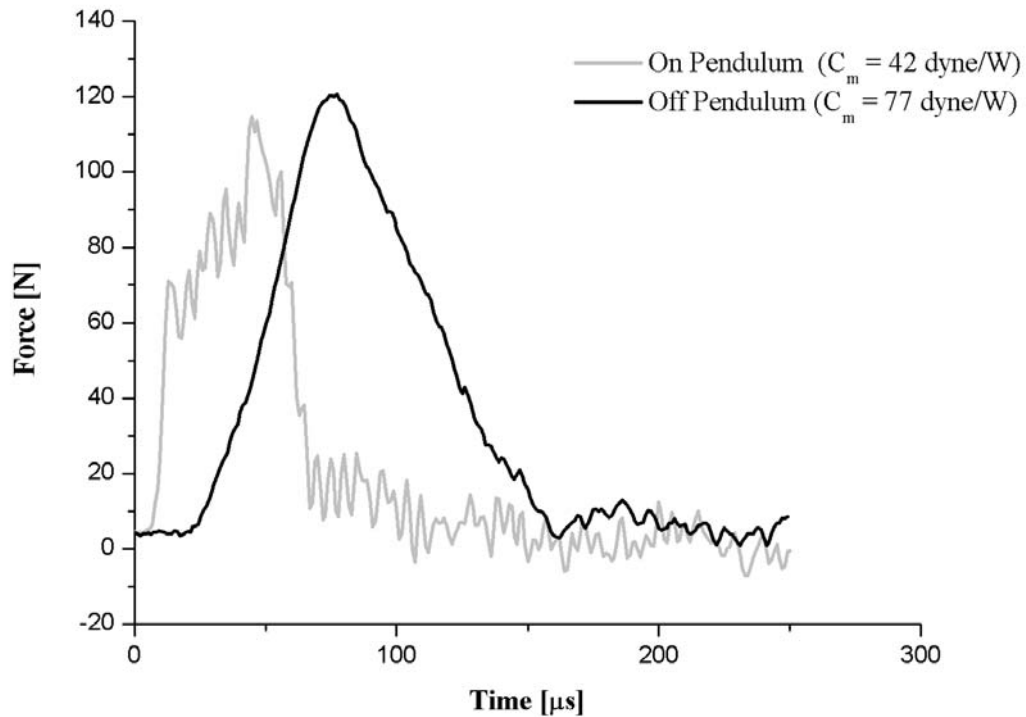

FIGURE 4. On- and off-pendulum impulse curves.

ICCD Imaging

ICCD images were taken of Delrin pellets during ablation. Laser fluence was 7 J/cm^2, with the beam spot size of approximately the same size as the target surface area. Figure 5 present the profile image sequences for white Delrin. Time delays counted from the arrival of laser pulse are given in the captions, while exposure times were kept at 10 ns.

In Figure 5 the images show the evident heating of the surface and initial plasma formation at A), further plasma plume development from B) to D), plume decoupling from the surface at E) and spherical expansion of hot vapors from G) to L). Note, for example, on image I), the target pellet, has been almost fully covered by this expanding vapor.

In effort to identify the physical process leading to the generation of thrust, the force-time curve for a white Delrin pellet shown in Figure 6 was compared to the sequence of images on Figure 5.

Figure 6 shows a smooth rise and decay curve, with duration of approximately15 μs. The thrust is being applied in the 5 – 12 μs interval, peaked at 13 μs after the arrival of

laser pulse. Comparison with Figure 5 indicates that the thrust is being produced during E-F-G sequence of images, centered at F. This period of time is characterized by a "mixed" behavior: the light-emitting plasma is seen together with opaque vapor (Figure 5, F).
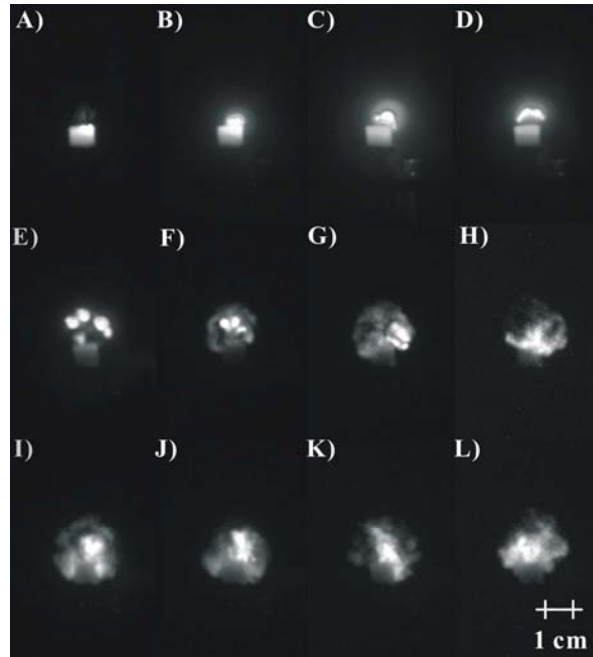

FIGURE 5. White Delrin image sequence. The delays are: A) 20 ns; B) 1 μs; C) 2 μs; D) 3 μs; E) 10 μs; F) 15 μs; G) 20 μs; H) 30 μs; I) 40 μs; J) 50 μs; K) 60 μs; L) 80 μs.
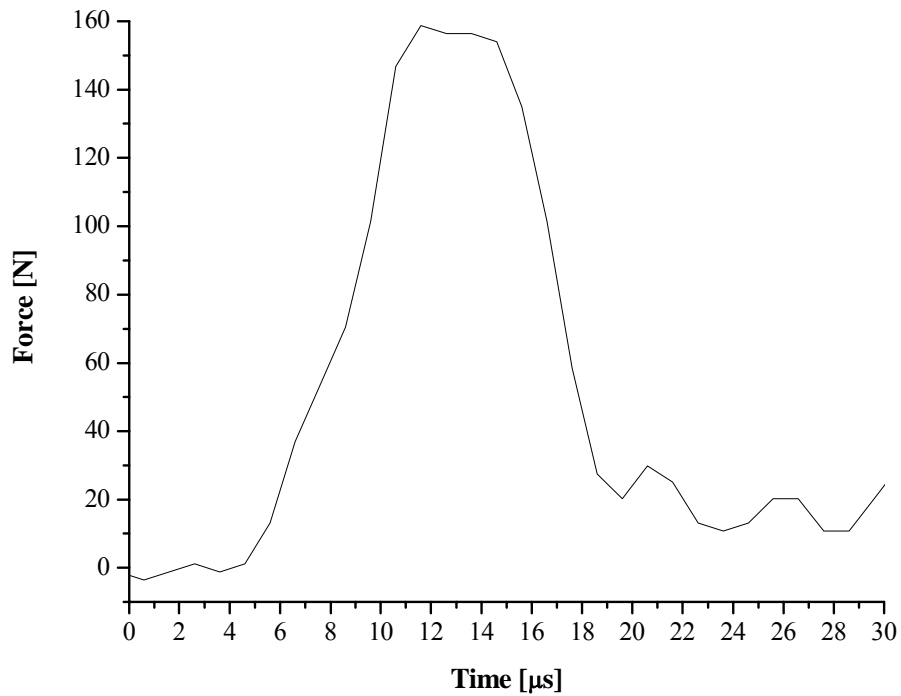

FIGURE 6. Force-time curve for white Delrin pellet. (Pulse energy: 10 J).

Figure 7 shows an image sequence for combustion process of white Delrin from 80 μs up to 5 ms time after the laser pulse arrival. The images were much dimmer than those presented on Figure 5. For this reason, in order to capture actual images of plume expansion, 10 μs exposure time was used.

As it can be discerned from presented images, at time when the combustion plume dominates the picture, the ablation plasma, air breakdown plasma, associated shockwaves and intense laser-induced vaporization processes have already ceased. As the images show, after 200 μs the combustion plume is fully decoupled from the target surface.
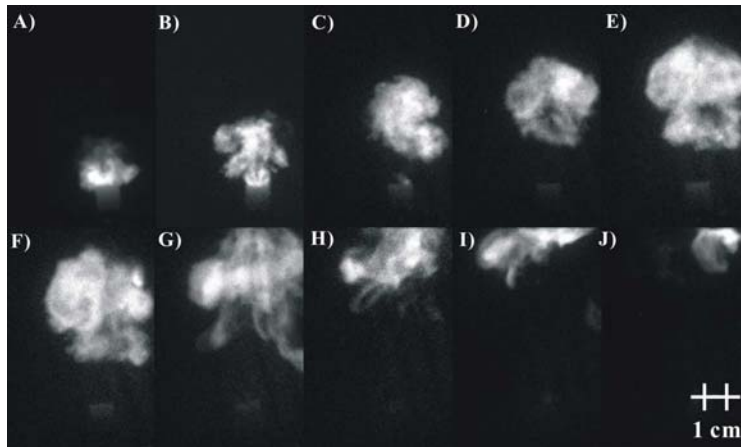

FIGURE 7. Combustion image sequence. A) 80 μs; B) 200 μs; C) 400 μs; D) 600 μs; E) 800 μs; F) 1 ms; G) 2 ms; H) 3 ms; I) 4 ms; J) 5 ms.
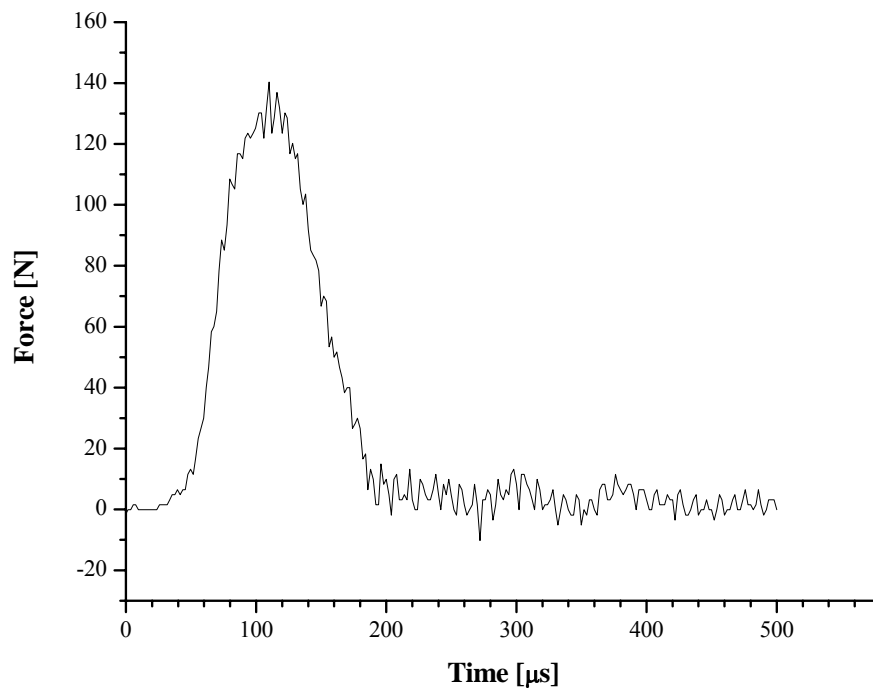

FIGURE 8. 16:1 thruster, white Delrin

Mini Thruster Measurement of C_m

In the previous section we had described the thrust, generated on irradiated propellant pellets "as is", *i.e.* without mini-thruster. This section presents the results of the similar measurements, performed on polymer propellants placed within the thrusters. Force-time curves were integrated to obtain impulse, and from this value, coupling coefficient was derived.

In all cases an addition of the thruster led to substantial extension of time over which the thrust was imparted, while the peak force was approximately the same. As an example, compare Figures 6 and 8 for white Delrin. When the thruster was used, the force-time curve spans almost 200 μs, as seen in Figure 8 for white Delrin, which is almost 10 times greater than for the bare propellant pellet (Figure 6).

Table 2 shows the coupling coefficients derived for white Delrin, black Delrin, and PVC for both tested thruster expansion ratios. The largest coupling coefficient (51 dyne/W) is achieved on white Delrin with the 16:1 expansion ratio thruster. In all cases (including least pronounced black Delrin), the 16:1 expansion ratio led to a greater coupling coefficient comparing to 8:1 thruster. White Delrin leading the C_m table, is followed by black Delrin and PVC.

TABLE 2. Coupling coefficients and specific impulses for Delrin and PVC.

	Exp. Ratio	Impulse [dyne-s]	C_m [dyne/W]
Black Delrin	*16:1*	818	38
	8:1	769	36
White Delrin	*16:1*	1089	51
	8:1	726	34
PVC	*16:1*	450	21
	8:1	398	18

Temporal Resolution of Plasma Shielding

Using the setup shown in Figure 3, we did transmission measurements of temporal profiles for beams passing through the pinhole in propellant pellet. The measurements were performed for aluminum and black Delrin and compared with the free-passing beam profile. The results are presented in Figure 9.

As Figure 9 shows, the free-passing laser pulse profile extends well into 2 μs. Furthermore, it can be seen that the Delrin and aluminum pulse profiles are cut off after about 85 ns. This indicates that plasma reaches the critical density within this time interval (85 ns) and stays in this condition over the rest of the pulse. Therefore, losses approaching ~ 90% of pulse energy occur due to plasma reflection. This is yet another indication that shorter pulses (like those employed for Ablative Laser Propulsion) are more efficient for laser propulsion [11].
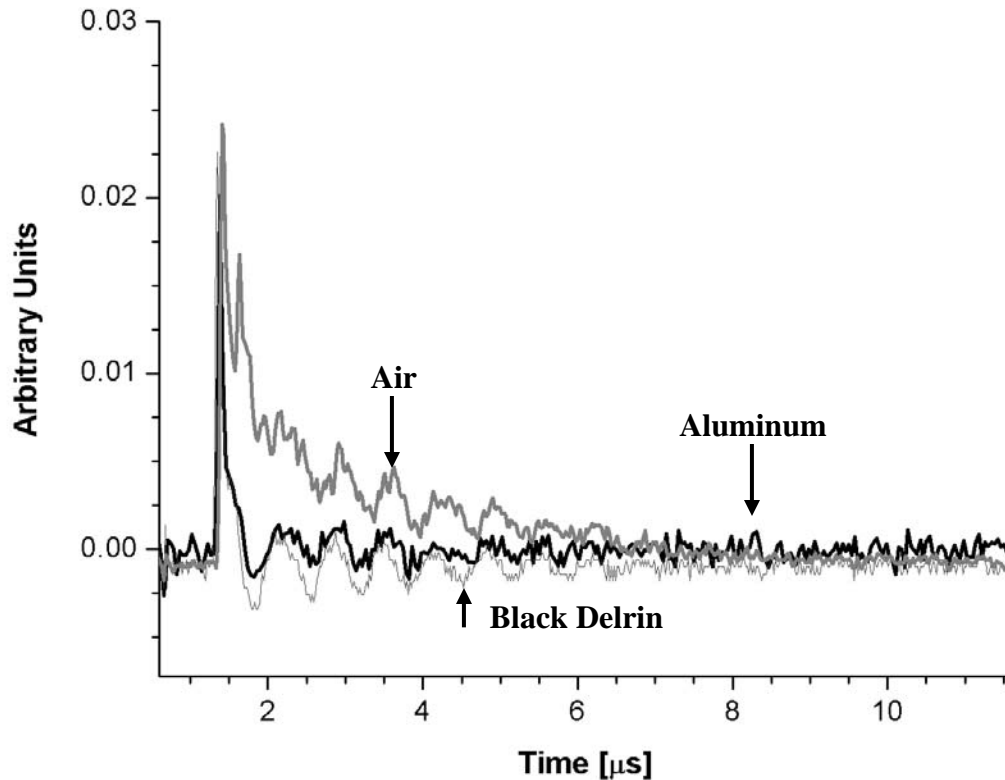
FIGURE 9. Laser pulse temporal profiles transmitted through a pinhole in propellant pellet *vs*. free-space profile.

Combustion Effects

The force-time curves for white Delrin in the 16:1 thruster were taken in air and in nitrogen atmosphere and compared. Pressure in the chamber was set at 1 atmosphere of nitrogen. The curves are shown in Figure 10.

On Figure 10 two curves appear to have close areas. The thrust generated in air systematically exceeded the thrust generated in nitrogen atmosphere on ~ 12%, which shows the similarly increasing trend of combustion effect as it was reported earlier for Myrabo Laser Lightcraft and German lightcraft [7]. According to the imaging data (Figures 5 and 7), the combustion plume appears much dimmer than the plasma at early phase (Figure 5); the predominantly combustion plume (Figure 7) appears at much later phase (> 200 μs), than presented thrust peak (Figure 6). Although we can state that the combustion did not appear as a drastic contributor to the overall thrust as it was compared to the previous results [7], this experiment still served as a major, but not the sole indication that the combustion is a source of thrust.
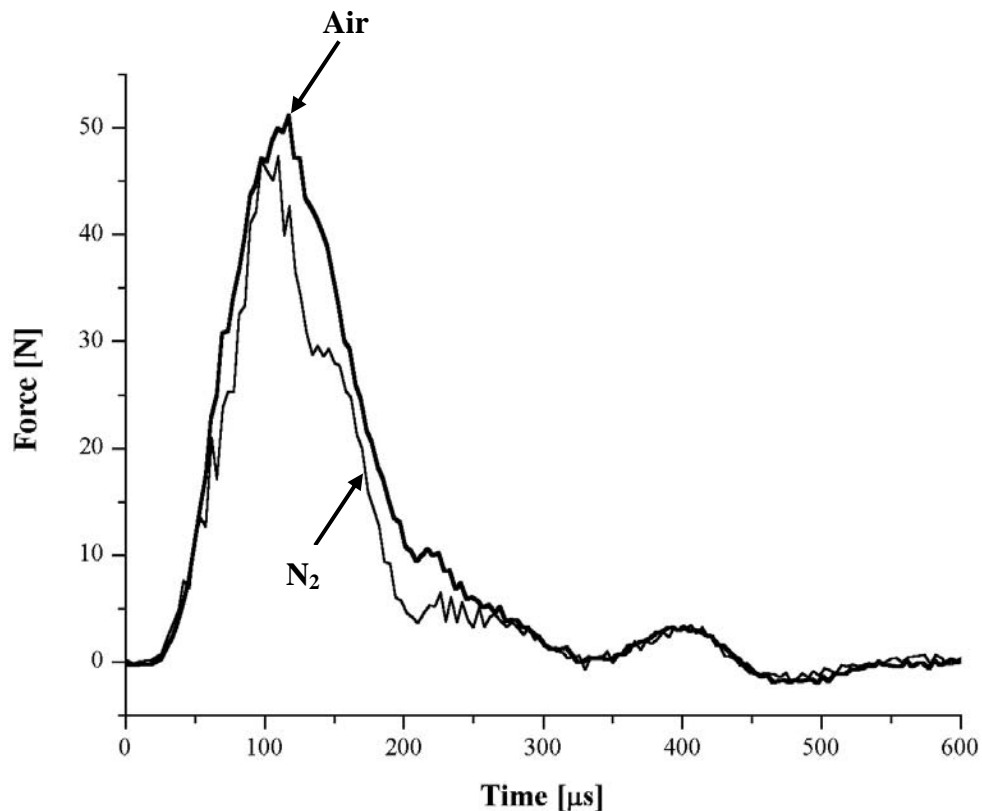
FIGURE 10. Force-time curves in air and nitrogen atmospheres, white Delrin.

CONCLUSIONS

A set of impulse measurements was conducted on polymers (white and black Delrin, PVC) propellant samples, placed within and without conical mini-thrusters of 8:1 and 16:1 expansion ratios. The major results were as followed:

1. The results from ballistic pendulum measurements and force-time curves were in good agreement, within the recoil correcting factor of 1/2. The force sensor measurements, when mounted on a stationary reference, resulted in an impulse value twice as large due the addition of recoil impulse.
2. On the polymers, ICCD imaging revealed 3 consequent phases. The first phase, lasted over $0 - 20$ μs period presented the energy deposition on the target causing plasma formation and expansion. The second phase, which lasts over $20 - 100$ μs is the shock wave expansion / vaporization / combustion, The third phase is the development of a combustion plume, which may reach out to 5 cm from the target and lasts for up to 5 ms.
3. Comparison of time-resolved imaging and force curves indicates that most likely the maximum impulse is imparted during the second phase. Comparison only adds limited impulse.

4. The coupling coefficients were highest on white Delrin (51 dynes/W), followed by black Delrin, and PVC. The measurements of force-time curves for the various types of propellants and two expansion ratios of thrusters shows consistently that the 16:1 thrusters provide higher coupling. The use of thruster leads to about an order of magnitude increase of time over which the impulse is imparted, while the peak force remains the same. Thus, for the propellants within the thrusters the time is ~ 150 μs compared to the bare pellets ~ 20 μs.

5. Finally, we have studied effects of plasma reflection, *i.e.* cut-off times when breakdown/ablation plasma becomes completely impenetrable for the laser pulse. The study shows a characteristic value for both black Delrin. Plasma reflection leads to ~ 90% loss of pulse energy.

ACKNOWLEDGEMENTS

REFERENCES

1. E. Sterling, A.V. Pakhomov, C.W. Larson and F.B. Mead, Jr., "Ablation of Absorption-Enhanced Water for Propulsion with TEA CO_2 Laser," Third International Symposium on Beamed Energy Propulsion, Troy, NY, 2004, edited by Andrew V. Pakhomov and Leik N. Myrabo, American Institute of Physics Conference Proceedings **766**, 474-481 (2005).

2. A.V. Pakhomov, J. Lin, and R. Tan, "Air pressure effect on propulsion with TEA CO_2 laser," accepted for publication in AIAA Journal.

3. A.V. Pakhomov, J. Lin, and K.A. Herren, "Effect of air pressure on propulsion with TEA CO_2 laser," High-Power Laser Ablation V, April 2004, Taos, NM, Proceedings of SPIE, edited by Claude R. Phipps, Vol. 5448, Part 2, 1017-1027 (2004).

4. A.V. Pakhomov and J. Lin, "Angular Distributions of Plasma Edge Velocity and Integrated Intensity: Update on Specific Impulse for Ablative Laser Propulsion," Third International Symposium on Beamed Energy Propulsion, Troy, NY, 2004, edited by Andrew V. Pakhomov and Leik N. Myrabo, American Institute of Physics Conference Proceedings **766**, 414-422 (2005)

5. Franklin B. Mead, Jr. and C.W. Larson, "Laser-Powered, Vertical Flight Experiments at the High Energy Laser System Test Facility," 36th AIAA/ASME/SAE/ASEE Joint Propulsion Conference and Exhibit, paper AIAA 2001-3661.

6. Willy L. Bohn and Wolfgang O. Schall, "Laser Propulsion Activities in Germany," First International Symposium on Beamed Energy Propulsion, Huntsville, AL, 2002, edited by Andrew V. Pakhomov, American Institute of Physics Conference Proceedings **664**, 79-91 (2003)

7. Wolfgang O. Schall, Hans-Albert Eckel, and Sebastian Walther, "Lightcraft Impulse Measurements under Vacuum," Special Report, DLR-German Aerospace Center, Institute of Technical Physics, Germany (2003)

8. A.V. Pakhomov, M.S. Thompson, and D.A. Gregory, "Ablative Laser Propulsion Efficiency," Presented at 33rd AIAA Plasmadynamics and Lasers Conference, 20 - 23 May 2002, Maui, Hawaii, AIAA Paper #2002-2157.

9. George P. Sutton, Rocket Propulsion Elements: An Introduction to the Engineering of Rockets, Sixth Edition, John Wiley & Sons, Inc., p418 (1992)

10. A.V. Pakhomov, D.A. Gregory, and M.S. Thompson, *AIAA Journal* **40**, #5, 947-952 (2002).

11. A.V. Pakhomov, T. Cohen, J. Lin, M.S. Thompson, and K. Herren, "Ablative Laser Propulsion: An Update, Part I," Second International Symposium on Beamed Energy Propulsion, Sendai, Japan, 2003, edited by Kimiya Komurasaki, American Institute of Physics Conference Proceedings **702**, 166-177 (2004)